Benchmark experiment for electron-impact ionization of argon: Absolute triple-differential cross sections via three-dimensional electron emission images

Xueguang Ren,[1] Arne Senftleben,[1] Thomas Pflüger,[1] Alexander Dorn,[1] Klaus Bartschat,[2] and Joachim Ullrich[1]
[1]*Max-Planck-Institut für Kernphysik, Saupfercheckweg 1, D-69117 Heidelberg, Germany*
[2]*Department of Physics and Astronomy, Drake University, Des Moines, Iowa 50311, USA*
(Received 8 April 2011; published 31 May 2011)

Single ionization of argon by 195-eV electron impact is studied in an experiment, where the absolute triple-differential cross sections are presented as three-dimensional electron emission images for a series of kinematic conditions. Thereby a comprehensive set of experimental data for electron-impact ionization of a many-electron system is produced to provide a benchmark for comparison with theoretical predictions. Theoretical models using a hybrid first-order and second-order distorted-wave Born plus *R*-matrix approach are employed to compare their predictions with the experimental data. While the relative shape of the calculated cross section is generally in reasonable agreement with experiment, the magnitude appears to be the most significant problem with the theoretical treatment for the conditions studied in the present work. This suggests that the most significant challenge in the further development of theory for this process may lie in the reproduction of the absolute scale rather than the angular dependence of the cross section.

DOI: 10.1103/PhysRevA.83.052714 PACS number(s): 34.80.Dp

I. INTRODUCTION

Electron-impact ionization of atoms and molecules plays an important role in a wealth of areas in physics and chemistry, including mass spectrometry, the upper atmosphere, plasma processes, gas discharges, and radiation. Accurate cross sections are not only of fundamental importance for understanding the mechanism of the ionization process, but they are also required for many modeling applications, ranging from studies of fusion plasmas to investigations into radiation effects in materials science and medicine.

Kinematically complete experiments on single ionization of atoms, so-called (e,2e) experiments, measure the momentum vectors of all final-state continuum particles (the scattered and ejected electrons as well as the recoil ion), and hence triple-differential cross sections (TDCSs) are determined. Thereby (e,2e) studies serve as a powerful method for the investigation of the dynamics of quantum mechanical few-body interactions. Since the pioneering works of Ehrhardt *et al*. [1] and Amaldi *et al*. [2] more than 40 years ago, (e,2e) TDCSs have been extensively studied experimentally and theoretically for a broad range of targets and kinematic conditions. The most frequently studied experimental collision geometry is the so-called coplanar geometry, in which both final-state electrons move in the plane that also contains the incoming projectile momentum.

In recent years, theory has made tremendous progress in describing the collision dynamics. The agreement between theoretical predictions and experiment has been steadily improving, especially for the fundamental target of atomic hydrogen, which is claimed to have been numerically solved with nonperturbative approaches such as (i) exterior complex scaling (ECS) [3,4], (ii) convergent close coupling (CCC) [5], and (iii) time-dependent close coupling (TDCC) [6]. As the next step, the process of electron-helium scattering has also been described very well in both CCC and TDCC calculations. See, for example, Refs. [7–9].

For heavier many-electron targets, on the other hand, the present situation is not as satisfying as for the simpler targets of atomic hydrogen and helium. The nonperturbative methods mentioned above are currently not applicable to carry out highly accurate computations for targets such as argon. The CCC method has recently been extended to the calculation of *s*-orbital ionization of neon and argon [10–12], but it is not yet applicable to calculations that involve ionization of electrons from a *p* shell. Currently, the electron-argon scattering process has to be treated at least to some extent perturbatively, usually within the distorted-wave Born approximation (DWBA) [13–17]. A hybrid approach [12,18–20], in which the interaction of a (fast) projectile is treated perturbatively while the scattering of the (slow) ejected electron from the residual ion is described through an *R*-matrix (close-coupling) expansion, has had some success, although the method is likely going to have problems when the projectile energy is lowered, the detection angle of the faster of the two outgoing electrons is increased, and the energy sharing is not highly asymmetric.

Experimentally, single ionization of argon has been extensively studied in the coplanar geometry in the intermediate- to high-energy regime. Here the agreement between theoretical predictions and experiment is found to be generally good concerning the relative shape, i.e., the angular dependence, of the cross sections, see e.g., Refs. [16–18,21,22]. One of the well-known outstanding issues in experiment, however, is the general lack of absolute cross-section data for ionization of the heavier targets. Recently, absolute (e,2e) measurements on neon and argon were reported by Hargreaves *et al*. [10] for the coplanar geometry. While a number of theories showed rather good agreement regarding the relative angular dependence of the cross section, the predicted magnitudes sometimes differed by up to a factor of 3 from each other and experiment. Moreover, three-dimensional (3D) (e,2e) cross-section results for argon were reported by Ren *et al*. [23], who observed significant discrepancies between experiment and theory for electron emission out of the scattering plane.

Therefore, a comprehensive experiment with absolute TDCSs via three-dimensional (3D) images for electron emission is urgently required to thoroughly assess the reliability of

theoretical predictions. In this paper, absolutely normalized 3D cross sections for argon $3p$-obital single ionization by 195-eV electron impact are presented for projectile scattering angles $\theta_1 = -5°$, $-10°$, $-15°$, and $-20°$, respectively, and for ejected electron energies $E_2 = 10$, 15, and 20 eV. The experimental 3D TDCSs and a series of cross-section cuts in the xy plane, yz plane, and xz plane within the laboratory frame, as indicated in Fig. 1(c) below, are compared to the theoretical predictions obtained by hybrid first-order and second-order distorted-wave Born plus R-matrix (close-coupling) approaches (DWB1-RM and DWB2-RM).

II. EXPERIMENT

The present experiments were performed with an advanced reaction microscope that was especially designed for electron-impact experiments [24]. Details of the experimental setup and the procedure were described elsewhere [23], [25]. Very briefly, a pulsed electron beam crosses an argon supersonic gas jet and causes the ionization of one bound electron from the target. Using uniform electric and magnetic fields, the fragments in the final state (two electrons and the recoil ion) are projected onto two position- and time-sensitive multihit detectors. From the positions of the hits and their times of flight, the vector momenta of the detected particles can be calculated. Experimental data were obtained with the triple-coincidence detection of two outgoing electrons (e_1 and e_2) plus the recoil ion. The momentum vectors of the two outgoing electrons were measured directly without relying on the recoil-ion momentum. This allows for (e,2e) studies on heavy and warm targets with the reaction microscope. The absolute scale of the cross section was obtained by normalizing to the absolute measurements in the coplanar geometry by Hargreaves *et al.* [10]. It should be noted that all data in the present experiment were recorded simultaneously in a single run. Consequently, once the normalization factor has been fixed for one point, the cross sections for all other geometries are internormalized across all recorded scattering angles and all ejected electron energies.

III. THEORY

DWB1-RM and DWB2-RM have been described in detail in several earlier publications, e.g., Refs. [12], [18], and [26]. Briefly, the interaction of a (fast) projectile with the target is treated perturbatively to first or second order, with additional approximations being needed to make the second-order treatment numerically possible. On the other hand, the scattering of the (slow) ejected electron from the residual Ar^+ ion is described through an R-matrix (close-coupling) expansion. Specifically, it has been shown that a two-state approximation, coupling only the final ionic states $(3s^2 3p^5)^2 P$ and $(3s3p^6)^2 S$, respectively, is generally sufficient for this part of the problem. In addition to accounting for the most important channel-coupling effects, it is worth noting that these models employ accurate multiconfiguration expansions of both the final ionic states and the initial $(3s^2 3p^6)^1 S$ bound state, namely, those developed by Burke and Taylor [27]. This, by itself, is a significant improvement over typical distorted-wave treatments that would only use single-configuration descriptions and a single $3p$ orbital, in fact, the same orbital for the initial neutral and the final ionic states. As mentioned previously, the hybrid model was designed for highly asymmetric kinematics, and hence problems of increasing magnitude can be expected when going away from this limitation.

IV. RESULTS AND DISCUSSION

Figure 1 exhibits the absolute 3D TDCSs for the argon $3p$ orbital ionization for scattering angles of $\theta_1 = -5°$, $-10°$, $-15°$, and $-20°$ of the fast final-state electron as a function of the emission angle of the slow ejected electron with energy $E_2 = 10$ eV. The projectile is coming in from the bottom ($\vec{k}_0$) and is scattered to the left ($\vec{k}_1$), as indicated in Fig. 1(c). These two vectors define the scattering (yz) plane shown in Fig. 1(c). The 3D TDCS for a particular direction is given as the distance

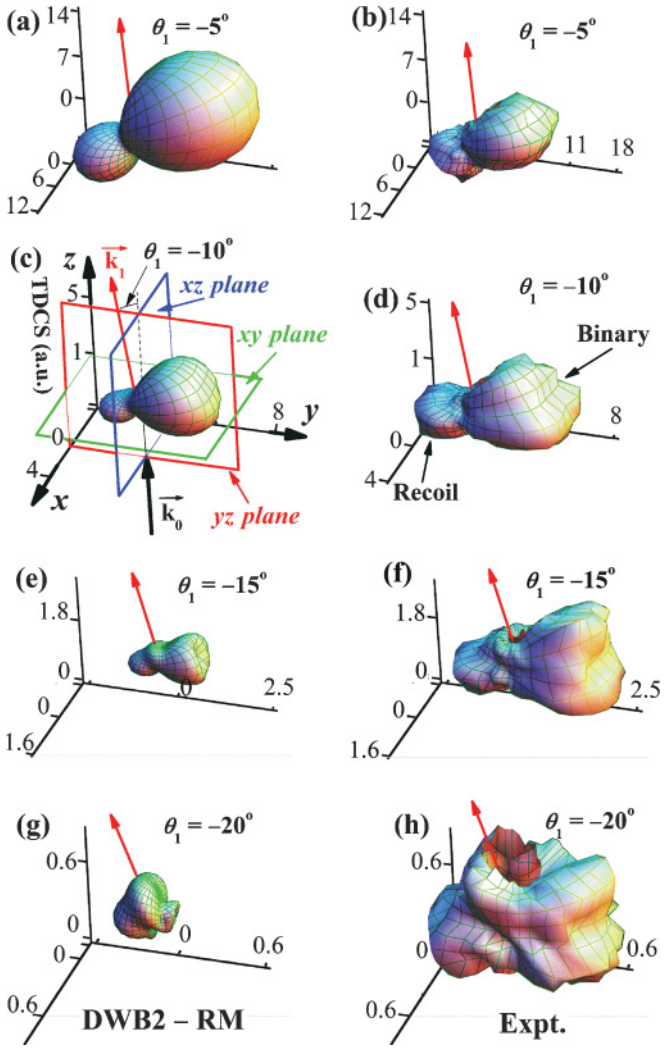

FIG. 1. (Color online) Absolute 3D TDCS, in atomic units, for argon $3p$ orbital ionization by 195-eV electron impact as a function of the low-energy ($E_2 = 10$ eV) electron emission angle. From the top to bottom row the projectile scattering angle θ_1 is fixed to (a) and (b) $\theta_1 = -5°$, (c) and (d) $\theta_1 = -10°$, (e) and (f) $\theta_1 = -15°$, and (g) and (h) $\theta_1 = -20°$. Left-hand column: the DWB2-RM predictions. Right-hand column: Experiment. The results in (e) and (f) were also presented in Ref. [23], but only on a relative scale for the experimental data of (f).

from the origin of the plot (also corresponding to the collision point) to the point on the surface, which is intersected by the ionized electron's emission direction.

The experimental 3D TDCSs are governed by the well-known binary and recoil lobes. The binary lobes exhibit shallow minima for particular kinematic conditions, such as in Figs. 1(d) and 1(f). These minima are the characteristic feature for ionization of a p orbital close to Bethe ridge conditions where the transferred momentum is close to the ejected electron's momentum, as discussed in Ref. [23]. The relatively large cross section in the angular range between the binary and recoil lobes is also remarkable. Also included in Fig. 1 (left-hand column) are the theoretical predictions obtained with the DWB2-RM model. Regarding the general shape of the 3D TDCSs, the qualitative features observed in experiment are reasonably well reproduced by theory. However, the most significant issue is the predicted magnitude of the cross sections in comparison with the experiment. One can clearly see that the magnitude of the experimental cross section decreases when changing the scattering angle from $\theta_1 = -5^\circ$ to -20°. This decrease also occurs in the theoretical predictions, but the calculated decrease in magnitude is much more rapid than what is seen in the experimental data. The cross-section magnitude is overestimated by theory at the scattering angle of $\theta_1 = -5^\circ$, as seen in Figs. 1(a) and 1(b). For $\theta_1 = -15^\circ$ and -20°, on the other hand, the calculated magnitude is underestimated, as seen in Figs. 1(e)–1(h).

For more quantitative comparisons of experiment and theory, absolute TDCS cuts through the 3D images are presented in Fig. 2. The cross sections in the yz plane (left-hand column), the xz plane (central column), and the xy plane (right-hand column) are plotted as a function of

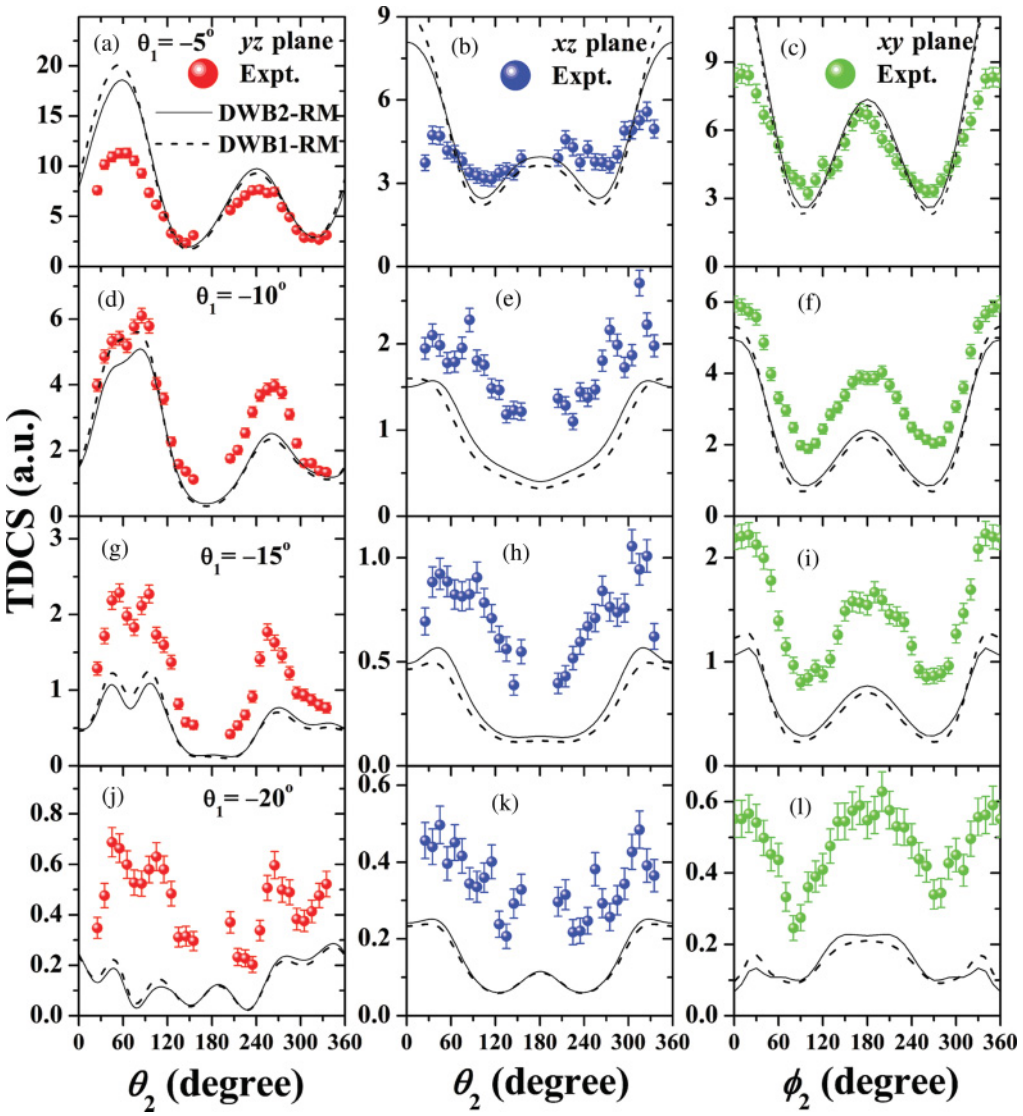

FIG. 2. (Color online) Absolute TDCS, in atomic units, presented as cuts through the 3D images shown in Fig. 1 as a function of the low-energy ($E_2 = 10$ eV) electron emission angle. From the top to bottom row the projectile scattering angle θ_1 is fixed to (a) to (c) $\theta_1 = -5^\circ$, (d)–(f) $\theta_1 = -10^\circ$, (g)–(i) $\theta_1 = -15^\circ$, and (j)–(l) $\theta_1 = -20^\circ$. Left-hand column: TDCS in the yz plane. Central column: TDCS in the xz plane. Right-hand column: TDCS in the xy plane, $\phi_2 = 0^\circ$ is corresponds to y axis. The results in (d) and (e) and (g) and (h) were also presented in Ref. [23], but only on a relative scale for the experimental data.

the ejected-electron ($E_2 = 10$ eV) emission angle at projectile scattering angles of $\theta_1 = -5^\circ$, -10°, -15°, and -20°. Also presented in Fig. 2 are the predictions from the DWB1-RM and DWB2-RM methods. Regarding the relative shape of the TDCSs, the calculations for the *yz* plane and *xy* plane are generally in reasonable agreement with the experimental data, although the discrepancies between experiment and theory become significant for the angular range of θ_2 close to 0° for $\theta_1 = -20^\circ$, as seen very clearly in Fig. 2(j). This may be attributed to the post-collision interaction (PCI) being neglected in the model. In the *xz* plane, even the relative shape is not well reproduced by the theory. For example, the observed double-peak structure, which is closely related to the binary lobe feature, is not reproduced by the calculations. A possible source for this discrepancy may be higher-order projectile-nucleus interactions, as previously discussed in Ref. [23].

As expected from Fig. 1, the most distinct difference between theory and experiment concerns the magnitude of the cross sections. It is found that the predicted magnitude is overestimated by a factor of 2 for $\theta_1 = -5^\circ$ but underestimated by a factor up to 3 for the cases of $\theta_1 = -15^\circ$ and -20°. The precise cause of this issue is unknown at the present time, since several approximations—none of which can currently be lifted—are made in the theory. These findings certainly suggest that significant further theoretical developments are required to treat the various physical effects (electron exchange, channel coupling, and short-range and long-range correlations) more accurately in electron-impact ionization of many-electron systems.

Absolute TDCSs for the ejected electron energies of $E_2 = 15$ and 20 eV and projectile scattering angles $\theta_1 = -5^\circ$, -10°, -15°, and -20° are presented in Fig. 3. Also included in the figure are the DWB2-RM results. It can be seen that the difference of the cross-section magnitude between the ejected-electron energies of $E_2 = 15$ and 20 eV (for the same scattering angle) is relatively larger at the scattering angle of $\theta_1 = -5^\circ$ (the top row in Fig. 3) than in the case of $\theta_1 = -20^\circ$ (the bottom row in Fig. 3). This observation is consistent

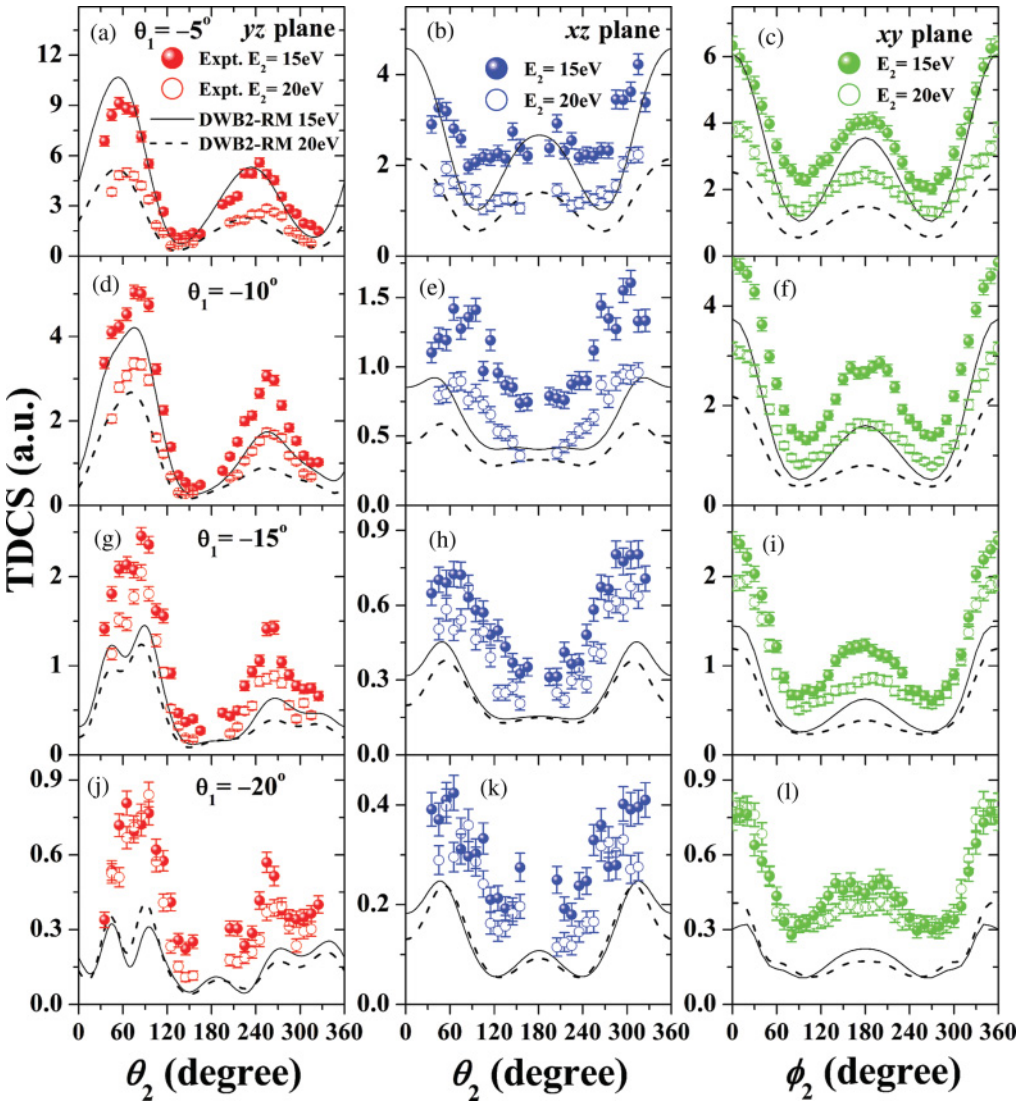

FIG. 3. (Color online) Same as Fig. 2 but for the ejected electron energies of $E_2 = 15$ and 20 eV. The results for the ejected electron energy of $E_2 = 15$ eV in (a) and (b), (d) and (e), and (g) and (h) were also presented in Ref. [23], but only on a relative scale for the experimental data.

with the theoretical prediction from the DWB2-RM model. It is found once again that the relative angular dependence of the cross section is reasonably well reproduced by theory, with the remaining discrepancies probably being due to the PCI effect and higher-order projectile-nucleus scattering mentioned above. The most significant issue with the theory remains the predicted magnitude of the cross sections. The differences between theory and experiment reach up to a factor of 3 for the kinematic condition of $\theta_1 = -20^\circ$, as shown in the bottom row of Fig. 3.

V. SUMMARY

A comprehensive experimental investigation of electron-impact ionization of the many-electron argon target has been reported. In order to assess the state of theoretical predictions, absolute triple-differential cross sections for electron emission in a series of collision kinematics were presented via three-dimensional images as well as selected cuts through a few planes. The experimental data were compared with predictions from DWB1-RM and DWB2-RM hybrid models. The relative shape of the cross section was generally well reproduced by these models, though some discrepancies remained, especially for the cross section in the xz plane of the 3D pattern. The prediction of the cross-section magnitude, however, is the most significant issue with the current theory. It was found that the predicted magnitude of the cross sections may be overestimated by a factor of 2 at the kinematic condition of $\theta_1 = -5^\circ$ and $E_2 = 10$ eV or underestimated by a factor of 3 ($\theta_1 = -20^\circ$ and $E_2 = 10$ eV). These findings strongly suggest that the physics behind the electron-impact ionization of many-electron systems needs to be treated more accurately by theory.

The present investigation of absolute 3D cross sections provides a comprehensive test of theory. The DWB2-RM hybrid model can reproduce well the TDCSs both in the relative shape and the absolute scale for a few particular kinematic conditions. For example, the TDCS at $\theta_1 = -5^\circ$ and $E_2 = 20$ eV, as shown in Fig. 3(a), is well described by theory in the scattering (yz) plane. However, the good agreement vanishes at other kinematic conditions, such as the cross sections for emission out of the scattering plane shown in Figs. 3(b) and 3(c) and at other scattering angles and ejected-electron energies, for example, those depicted in Figs. 3(d)–3(i). Therefore, the present investigation clearly emphasizes that measurements including an absolute scale, a 3D electron emission pattern, and a series of collision kinematic conditions are necessary to thoroughly assess the state of theory in this field.

ACKNOWLEDGMENTS

X.R. acknowledges support from Deutsche Forschungsgemeinschaft (DFG) under project No. RE 2966/1-1. K.B. was supported by the United States National Science Foundation under Grant No. PHY-0757755.

[1] H. Ehrhardt, M. Schulz, T. Tekaat, and K. Willmann, Phys. Rev. Lett. **22**, 89 (1969).
[2] U. Amaldi, A. Egidi, R. Marconero, and G. Pizzella, Rev. Sci. Instrum. **40**, 1001 (1969).
[3] T. N. Resigno, M. Baertschy, W. A. Isaacs, and C. W. McCurdy, Science **286**, 2474 (1999).
[4] P. L. Bartlett, J. Phys. B **39**, R379 (2006).
[5] I. Bray, Phys. Rev. Lett. **89**, 273201 (2002).
[6] J. Colgan and M. S. Pindzola, Phys. Rev. A **74**, 012713 (2006).
[7] J. Colgan, M. Foster, M. S. Pindzola, I. Bray, A. T. Stelbovics, and D. V. Fursa, J. Phys. B **42**, 145002 (2009).
[8] I. Bray, D. V. Fursa, A. S. Kadyrov, and A. T. Stelbovics, Phys. Rev. A **81**, 062704 (2010).
[9] X. Ren, I. Bray, D. V. Fursa, J. Colgan, M. S. Pindzola, T. Pflüger, A. Senftleben, S. Xu, A. Dorn, and J. Ullrich, Phys. Rev. A **83**, 052711 (2011).
[10] L. R. Hargreaves, M. A. Stevenson, and B. Lohmann, J. Phys. B **43**, 205202 (2010).
[11] A. Naja, E. M. Staicu Casagrande, A. Lahmam-Bennani, M. Stevenson, B. Lohmann, C. Dal Cappello, K. Bartschat, A. Kheifets, I. Bray, and D. V. Fursa, J. Phys. B **41**, 085205 (2008).
[12] K. Bartschat, D. V. Fursa, and I. Bray, J. Phys. B **43**, 125202 (2010).
[13] I. E. McCarthy, Z. Phys. D **23**, 287 (1992).
[14] X. Zhang, C. T. Whelan, and H. R. J. Walters, Z. Phys. D **23**, 301 (1992).
[15] A. Prideaux and D. H. Madison, Phys. Rev. A **67**, 052710 (2003).
[16] A. Prideaux, D. H. Madison, and K. Bartschat, Phys. Rev. A **72**, 032702 (2005).
[17] A. S. Kheifets, A. Naja, E. M. Staicu Casagrande, and A. Lahmam-Bennani, J. Phys. B **41**, 145201 (2008).
[18] K. Bartschat and O. Vorov, Phys. Rev. A **72**, 022728 (2005).
[19] K. Bartschat and P. G. Burke, J. Phys. B **20**, 3191 (1987).
[20] K. Bartschat and P. G. Burke, J. Phys. B **21**, 2969 (1988).
[21] K. D. Winkler, D. H. Madison, and H. P. Saha, J. Phys. B **32**, 4617 (1999).
[22] B. Rouvellou, S. Rioual, J. Röder, A. Pochat, J. Rasch, C. T. Whelan, H. R. J. Walters, and R. J. Allan, Phys. Rev. A **57**, 3621 (1998).
[23] X. Ren, A. Senftleben, T. Pflüger, A. Dorn, K. Bartschat, and J. Ullrich, J. Phys. B **43**, 035202 (2010).
[24] J. Ullrich, R. Moshammer, A. Dorn, R. Dörner, L. Ph. H. Schmidt, and H. Schmidt-Böcking, Rep. Prog. Phys. **66**, 1463 (2003).
[25] M. Dürr, C. Dimopoulou, A. Dorn, B. Najjari, I. Bray, D. V. Fursa, Z. Chen, D. H. Madison, K. Bartschat, and J. Ullrich, J. Phys. B **39**, 4097 (2006).
[26] M. Stevenson, G. J. Leighton, A. Crowe, K. Bartschat, O. K. Vorov, and D. H. Madison, J. Phys. B **38**, 433 (2005); **40**, 1639 (2007) (corrigendum).
[27] P. G. Burke and K. T. Taylor, J. Phys. B **8**, 2620 (1975).